Engineering and Technology Journal
Journal homepage: https://etj.uotechnology.edu.iq

Optimization Process of Double Spots Welding of High Strength Steel Using in the Automotive Industry

Hayder H. Khaleel[a,b*], **Ibtihal A. Mahmood**[b], **Fuad Khoshnaw**[c]

[a] Mechanical Engineering Dept, University of Technology-Iraq, Alsina'a Street, 10066 Baghdad, Iraq.
[b] Engineering Technical College / Najaf, Al- Furat Al-Awsat Technical University, 31001 Al-Najaf, Iraq.
[c] De Montfort University, United Kingdom.
*Corresponding author Email: me.19.32@grad.uotechnology.edu.iq

HIGHLIGHTS

- Double spot welding for high-strength low alloy steel which is a new steel grade.
- The results showed that optimum welding parameters are welding current of 8800 Amp, welding time of 20 cycles, and electrode force of 1900 N.
- Pull out failure mode because of high plastic deformation.
- The shunt effect phenomenon influences the mechanical properties of double spot welding.

ARTICLE INFO

Handling editor: Jalal M. Jalil

Keywords:

Resistance Spot Welding, Taguchi method, High Strength Steel, Welding parameters, Failure mode.

ABSTRACT

Resistance Spot Welding (RSW) is one of the most important welding techniques used in the automotive industry because it is an economic process and is suitable for many materials. Many parameters affect the mechanical and microstructural properties of nugget formation and its strength, like welding current, electrode force, and welding time. Therefore, optimizing the RSW process to get the optimum welding parameters is necessary for automobile manufacturing companies. High-strength steel is widely used in the automotive industry because of its superior characteristics such as high strength-weight ratio, ductility, fatigue, and corrosion resistance. This paper presents an optimization process for RSW using the Taguchi method for high strength low alloy steel (HSLA) DOCOL 500 LA, considered a new steel grade. Two spots were used in this work. The mechanical and microstructural tests are achieved to get the maximum nugget strength, nugget diameter, different welding zones microstructures, microhardness values, and failure modes. The results showed that optimum welding parameters were welding current of 8800 Amp, welding time of 20 cycles, and electrode force of 1900 N. The failure mode for optimum conditions was a full pullout with tearing of the welded sheets because of high plastic deformation and absorbed energy. The maximum microhardness value is in the fusion zone, the heat-affected region, and finally, in the base material due to the nugget zone's rapid melting and solidification process.

1. Introduction

The vehicle body is manufactured from thin sheets joined together via the resistance spot welding process. Thousands of nuggets are found in the modern automobile structure [1]. During a car accident, the safety of the passengers depends on the automobile structure integrity, which largely depends on spot welding performance. Therefore, the quality and performance of spot welding must be considered to ensure the best safe design of the car [2,3]. High-strength steels have many significant characteristics, such as a high strength-weight ratio and fatigue resistance, so they are used in the automotive industry instead of mild steel to decrease the car's body weight and to improve fuel efficiency [4]. During resistance spot welding, the heat is produced because of the flow of high electrical current through the welding parts according to Joule law:

$$Q = I2\ R\ t \quad (1)$$

Where Q is generated heat, I is welding current, t is welding time, and R is resistance. The input heat causes to raise the temperature of the parts being welded and then melts the material and finally forms the welding nugget [5]. The failure mode

http://doi.org/10.30684/etj.2022.134325.1236
Received 18 June 2022; Accepted 06 September 2022; Available online 24 September 2022
2412-0758/University of Technology-Iraq, Baghdad, Iraq

of the resistance spot welding is the indicator of mechanical characteristics. The resistance spot welding mainly fails in two modes [6]:

- Interfacial mode: this failure mode significantly influences the crashworthiness of the vehicle. The fracture propagates through the nugget zone.
- Pullout mode: this failure occurs when the nugget is separated from one of the sheets. This fracture can happen in any welding region, such as base material, heat-affected zone, and nugget zone. This type of failure indicates high absorbed energy and high plastic deformation.

The quality of resistance spot welding depends on the welding parameters, such as welding current, welding time, and electrode force. Specifying the optimum value for these parameters is a common problem for automobiles industries companies. Finding the relationship between the optimum parameters and the strength of the welding nugget is very important for industrial applications [7]. Many methods have been used to optimize the three main welding parameters. These methods are useful to ensure good welding quality and reduce production costs, especially in the automotive industry. Taguchi design method is considered one of the best methods in the optimization process, which can reduce the number of experiments by rearranging the number of tests through an orthogonal array and specifying the most effective parameters [8]. Most researchers studied the optimization process for single overlap design for materials such as mild steel and stainless steel. Sabah Khammass Hussein and Osamah Sabah Barrak [9] studied the resistance spot welding parameters' influence on the strength of two materials, AA 6061-T6 and AISI 304L, with different thicknesses. Three values for welding parameters were used, and analyzed their effects using the design of experiments. The results showed that an increase in the welding current and the sheet thickness increased the strength of welded parts. In contrast, increasing the electrode force and welding time caused to decrease in the strength of welded parts. Hassoni et al. [10] analyzed the resistance spot welding and corrosion resistance of stainless steel AISI 316L by using different welding parameters such as welding time, welding current, electrode force, and squeeze time. The samples were investigated using a tensile shear test and a Scanning Electron Microscope (SEM) inspection. Design of experiments used to analyze the effects of welding parameters on the strength of specimens. They obtained the optimum values of welding parameters, and the SEM results showed that increased welding current and electrode force led to increased pitting. Nor Atirah Mat Yasin et al. [11]. Studied the optimization process for spot welding using various parameters such as welding current, welding time, and electrode force for low-carbon steel. The experiments were done according to Taguchi method L9. The optimum parameters were welding current 8 kA, welding time 10 cycles, and electrode force 2.3 KN. The most effective parameter in their study was electrode force. The main objective of this current study is to design the optimization process for resistance spot welding for high strength low alloy steel DOCOL 500 LA, a new steel grade used in the chassis of a modern car. The microstructure of base material and tensile test are achieved to obtain the mechanical properties and to specify the rolling direction. Taguchi method with L9 array was used to determine the most effective parameters between the main three welding parameters (welding current, welding time, and electrode force). A tensile shear test is carried out to obtain the strength of the nugget, absorbed energy, and failure mode. Field Emission Scanning Electron Microscopy (FESEM) is used to study the effect of the welding process on the microstructure of the wedding zones. A microhardness test is carried out to study the variation of mechanical properties through a small welding area.

2. Experimental Work

2.1 Material

The material used in this paper was High Strength Low Alloy Steel (HSLA) DOCOL 500 LA, which was provided by a Swedish company (SSAB) for steel manufacturing. The thickness of the material was 0.8 mm. The chemical composition for HSLA was obtained using Thermo ARL 3460 Optical Emission Spectrometer. The results of chemical composition are listed in Table 1.

The material provided by the SSAB company was received as a plate with dimensions (50 x50) cm. A tensile test was carried out for six samples with three angles (0^o, 45^o, 90^o) to specify a rolling direction. Two samples were used for each direction. The samples were manufactured using Electrical Discharge Machine (EDM) to get accurate dimensions and good finishing according to ASTM- E8 for metallic materials (shell type). The tensile test was achieved using (Tinius Olsen) which was connected to a computer with a maximum capacity of 50 KN and a strain rate of 2 mm/min. The results of the tensile test for HSLA are listed in Table 2.

2.2 Welding Process

This work considered the influence of various welding parameters such as welding current, welding time, and electrode force. The dimensions of the welded samples were selected according to ISO standards. The sample size was (165x45) mm, and the overlap length was 45 mm, as shown in Figure 1.

Table 1: The chemical composition for HSLA

C%	Mn%	Si%	S%	P%	Cr%	Ni%	Mo%	Al%	Cu%	Fe%
0.0922	1.33	0.39	0.0063	0.0165	0.0343	0.0358	0.0064	0.0449	0.0085	Bal.

Table 2: Mechanical Properties of HSLA

Specimen	Yield strength (MPa)	Maximum Tensile Strength (MPa)	Fracture strength (MPa)	Elongation %
0° (1)	549	691	677	23
0°(2)	548	689	676	22
90°(1)	518	663	656	22.4
90°(2)	516	665	655	22
45°(1)	501	637	606	27.2
45°(2)	504	635	603	26.4

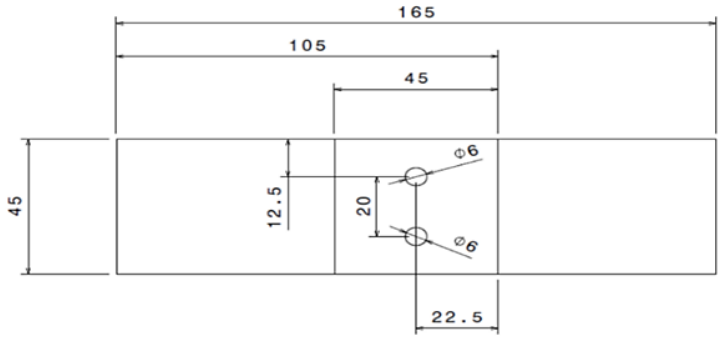

Figure 1: Dimensions of spot welding sample

The samples were cut using a CN machine to get the perfect shape and accurate dimensions. Then they were prepared with 0° angle to the rolling direction. After that, they were cleaned with artificial acetone to remove any dust or contaminations to ensure a good welding process. The welding process was done using a WIMTOUCH 1800 digital spot welding machine manufactured by welding industries Malaysia which was cooled by a water system. The electrode tip diameter was 6 mm, made of copper alloys selected according to the American welding society (AWS) standards. A special fixture was manufactured to hold the samples in the right position, as shown in Figure 2.

2.3 Design of Experiments

This research used three welding parameters to find the optimum shear strength. These parameters were welding current, welding time, and electrode force, with three levels for each parameter. These levels were selected according to AWS standards for high-strength steel materials with ultimate tensile strength from 350 MPa to 700 MPa. Taguchi method with L9 array was used, and analysis of the parameters using Minitab19 software. The welding parameters and levels are listed in Table 3.

The experiments showed that the welding current of less than 5700 Amp resulted in poor welding or lack of fusion, and more than 8800 Amp resulted in expulsion, and for the welding time, less than 9 cycles produced inappropriate penetration while more than 30 cycles resulted in expulsion. Therefore, the Taguchi method is a statistical and good optimization method with high efficiency of 95%. Nine samples were welded to obtain the tensile shear strength, absorbed energy, and specify the failure mode through the tensile shear test, as shown in Figure 3. In this research, it has focused on the tensile shear strength, so in the Taguchi method, the larger is better equation was selected:

$$\text{Larger is better S/N} = -10 \log (1/n \sum_{i=1}^{n} 1/y2) \quad (2)$$

Where S/N: Signal noise ratio; n: number of experiments; y: magnitude of the response

If it gets a maximum number for the tensile shear test, it indicates good tensile shear strength.

2.4 Tensile Shear Test

A tensile shear test was carried out to evaluate the strength of spot welding for nine specimens using a tensile test machine (SANTAM STD-600) with a maximum capacity of 600 KN. To increase the accuracy of tensile shear test results, the experiments were repeated two times and took the average result. The machine was connected to a computer to get a force-displacement curve with a strain rate of 1 mm/ min at room temperature, as shown in Figure 4.

The diameter and area of spot welding for all specimens were calculated using a visual measuring machine (VMM) connected to a computer and calibrated to obtain the accurate measurement of spot welding diameter, as shown in Figure 5.

2.5 Metallography

After the spot welding process was finished, the sample was cut using the EDM process from the centerline for a metallographic test. Then the cold mounting using the epoxy for which the resin to hardener ratio was 100:13 achieved. Then they were ground using different silicon papers (from grit 100 to grit 2000). The next step was to polish by alumina suspension and finally etch with Nital 2%. This etchant was composed of a 2% volume fraction of nitric acid in a 98% volume fraction of

alcohol (e.g., ethanol). Finally, the microstructure test was carried out for the base material as received before the welding process to specify the microstructure phase for HSLA. Moreover, the microstructure test was carried out for the sample after the spot welding process to examine the microstructure of the nugget zone, Heat Affected Zone (HAZ), and the base material to study the effect of welding parameters and rapid solidification on the microstructure of sample. Microstructure test was conducted using Optical Microscopy (Olympus BXM51), as shown in Figure 6, and Field Emission Scanning Electron Microscopy (FESEM) (TESCAN MIRA 3) was also used.

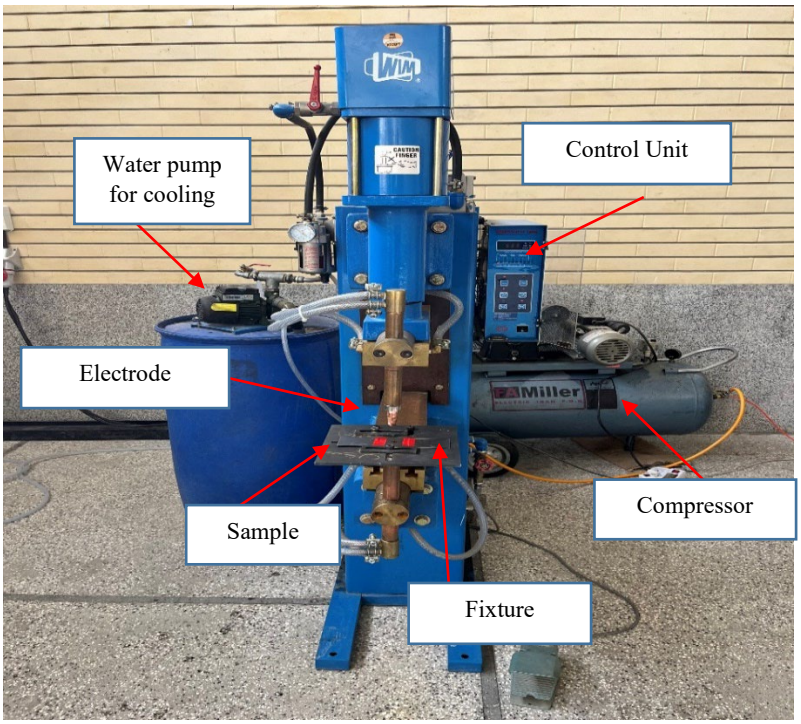

Figure 2: Spot Welding Machine

Table 3: Spot welding parameters

Parameter	Level 1	Level 2	Level 3
Current (Amp)	5700	7250	8800
Welding time (Cycle)	9	20	30
Force (N)	1900	2230	2560

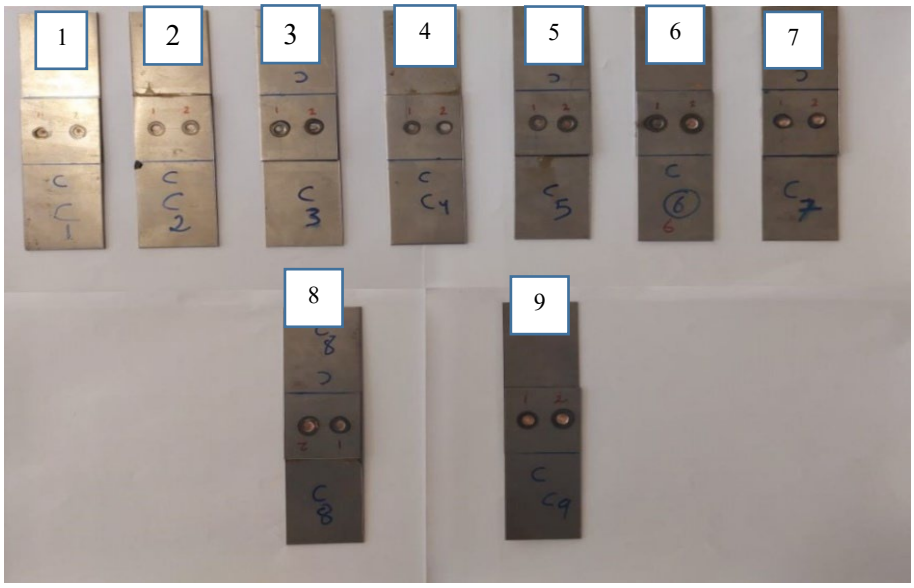

Figure 3: Nine samples with double spots

Figure 4: Tensile Shear Test

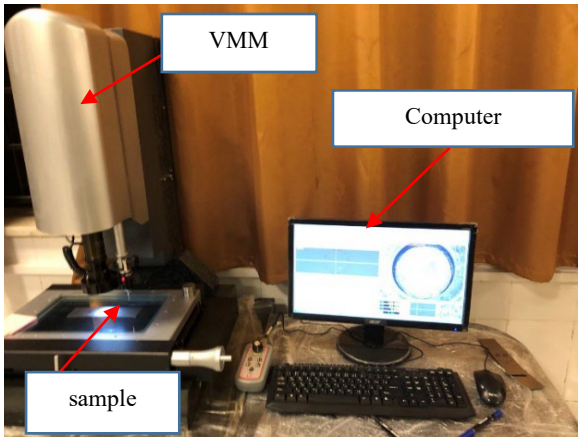

Figure 5: Visual Measuring Machine (VMM)

Figure 6: Optical Microscope (Olympus BXM51) equipped with digital camera and image processing software

2.6 Microhardness

The Vickers microhardness measurements were performed horizontally across the cross-section of the spot welds for three regions: the nugget zone, heat-affected zone, and base material for both spots for the welded sample with optimum welding parameters. The average microhardness of the base metal is 206 ± 3 HV. The preparation of samples included grinding and polishing according to ASTM E90-82. The test was carried out under load (500) gf and dwell time (10) s, as shown in Figure 7.

3. Results

3.1 Results of Tensile Shear Test

After the welding process was achieved, a tensile shear test was carried out for nine samples to get the maximum shear strength, absorbed energy, nugget diameter, and failure mode. The results are listed in Table 4.

It could be observed from the results that the tensile shear strength of spot welding increased by increasing the welding current, and this is due to the increase of the heat input to the sheets being welded, which increased the nugget area and subsequently increased the strength of the nugget. As a result, the maximum tensile shear strength is 18698 N, as shown in Figure 8.

It could be noticed that there is a difference between the diameter of nugget 1 and the diameter of nugget 2. This is because of a phenomenon called the shunting effect. In fact, previously made welds may influence the next nugget if the nuggets are spaced close to each other because of electric current shunting. The welding current may be diverted from the intended path by the previously made nugget. As a result, the current or current density may not be enough to produce a quality weld. The absorbed energy was calculated from the area under the force-displacement curve up to maximum force before failure occurred, as shown in Figure 9.

According to the Taguchi method, the optimum design was for current 8800 Amp, welding time 20 cycles, and for electrode force 1900 N as obtained from the analysis of S/N ratio using Minitab19 software as shown in Figure 10.

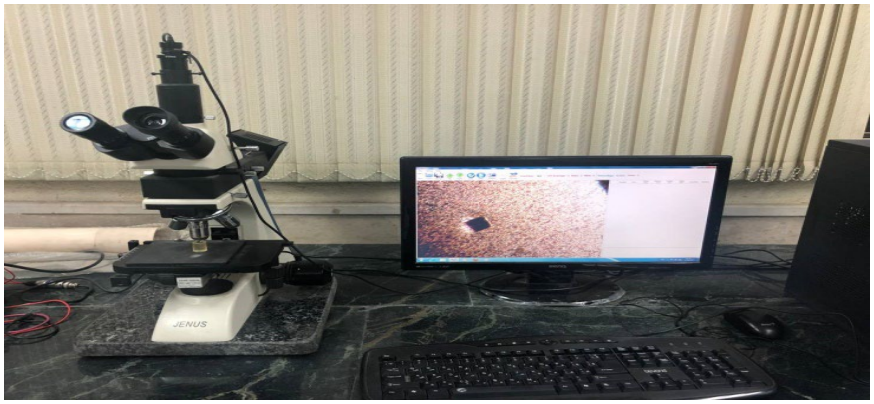

Figure 7: Microhardness Test

Table 4: Tensile Shear Test Results

Trail	Welding Current (Amp)	Welding Time (cycle)	Electrode Force (N)	Shear Force (N)	Absorbed Energy (J)	S/N ratio	Nugget Diameter 1 (mm)	Nugget Diameter 2 (mm)
1	5700	9	1900	13754	21.33	82.76	5.93	5.71
2	5700	20	2230	11183	7.97	80.97	6.41	6.28
3	5700	30	2560	10958	8.05	80.79	6.21	6.58
4	7250	9	2230	12665	13.79	82.05	6.30	6.71
5	7250	20	2560	17344	25.15	84.78	5.84	5.85
6	7250	30	1900	15137	27.12	83.60	6.52	6.69
7	8800	9	2560	17972	18.55	85.09	6.89	6.90
8	8800	20	1900	18776	44.03	85.47	6.87	6.83
9	8800	30	2230	18698	30.78	85.43	6.68	6.99

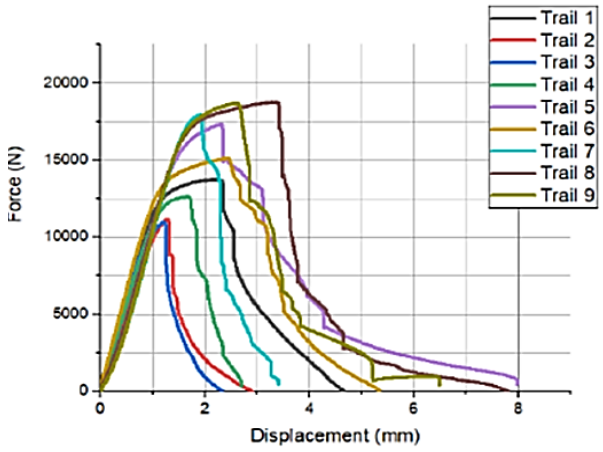

Figure 8: Tensile shear results

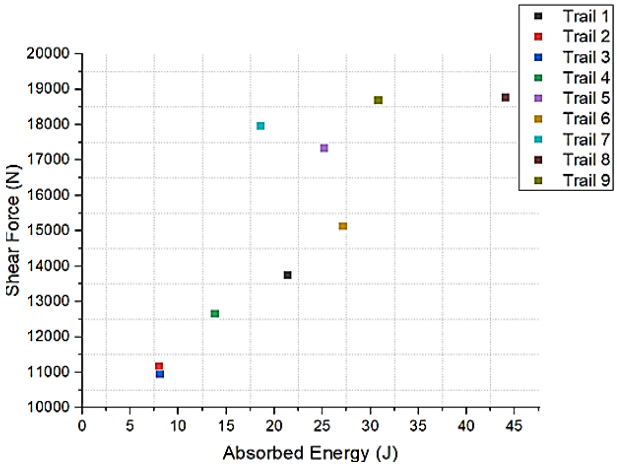

Figure 9: Tensile shear results

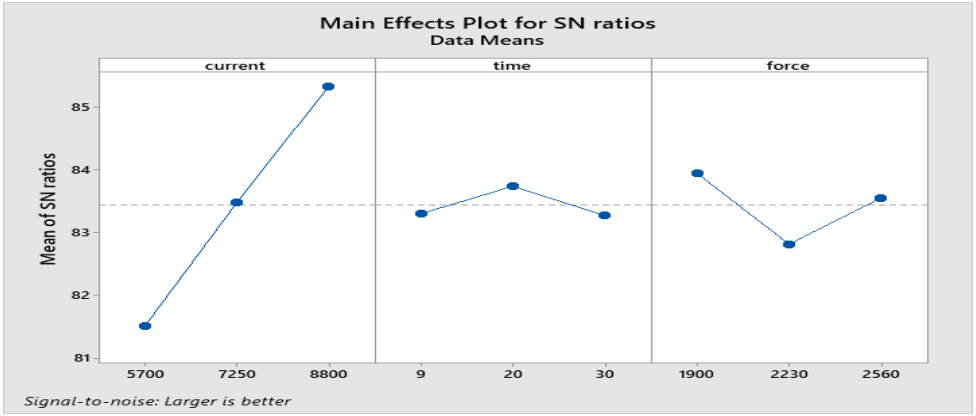

Figure 10: Main Effect plot for S/N ratio using Taguchi method

According to Taguchi, the predicted value for tensile shear strength was 19803 N. However, the confirmation test was carried out for two specimens, and the results for the first specimen were 18511 N with an error percentage of 6.5%. In contrast, the second specimen, 19139 N with an error percentage of 8.1%, and the variation was 1.7%, as shown in Figure 11. This variation is due to the welding defects such as microcracks and voids, which were affected by the results of the tensile shear test.

The failure mode is a pullout. For some samples was partial pullout, while for optimum samples was full pull out with tearing of the sheets due to high absorbed energy and high plastic deformation, as shown in Figure 12.

The most effective parameter is welding current, electrode force, and welding time, respectively obtained from the Taguchi method as listed in Table 5.

Figure 13 shows the Pareto charts. A Pareto chart is useful for analyzing the parameters affecting the spot welding process. The longer bar in the Pareto chart has the most significant, and it was the welding current.

The main goal of ANOVA is to study the effects of design parameters on the output results and their significant influence, as listed in Table 6.

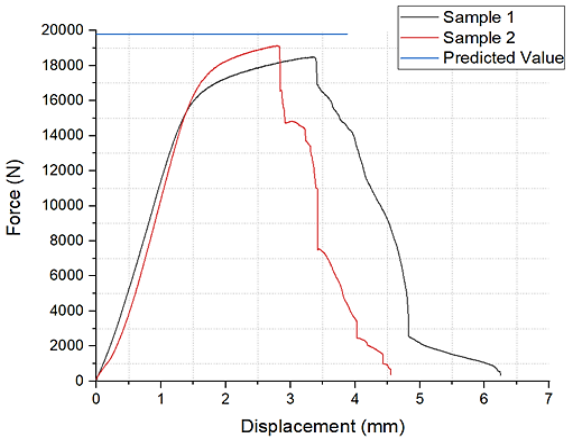

Figure 11: Confirmation test result

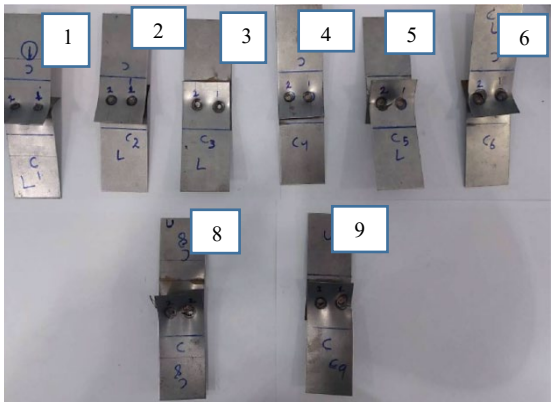

Figure 12: Samples after tensile shear test

Table 5: Response for signals to noise ratio

Level	Current	Time	Force
1	81.51	83.3	83.95
2	83.48	83.74	82.82
3	85.33	83.28	83.56
Delta	3.82	0.46	1.13
Rank	1	3	2

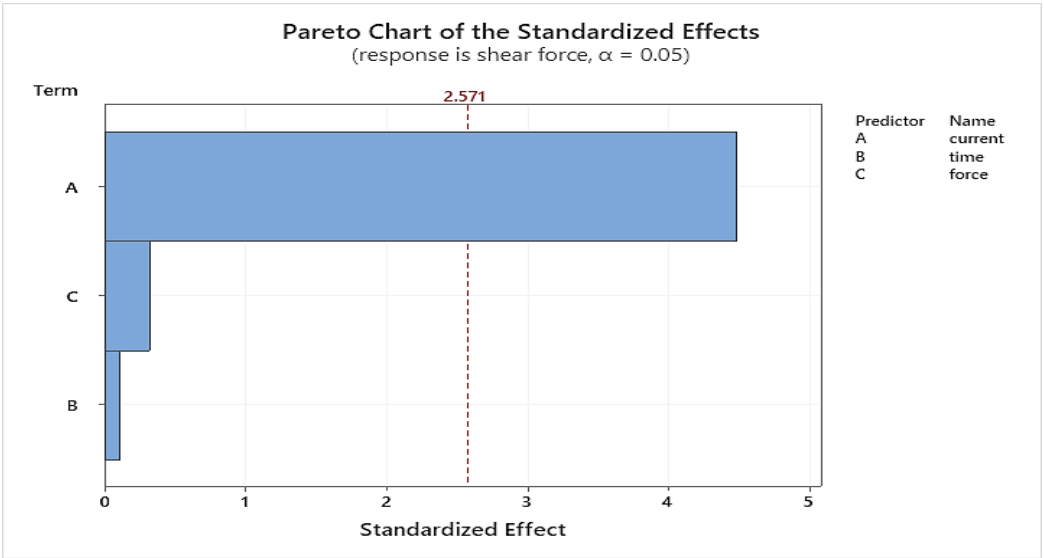

Figure 13: Pareto chart

3.2 Results of Microstructure and Microhardness Test

The microstructure was achieved using optical microscope for the base material before and after welding to specify the microstructure phase. It is well observed that the microstructure of the base material is almost completely ferritic with an equiaxed grain structure (i.e., having no certain shape and orientation). Then, the as-received material, according to the datasheet, was hot-rolled. In the hot rolling process, the material is expected to undergo dynamic recrystallization, producing a very fine equiaxed microstructure (in accordance with microstructural observations). As a result, the average grain size of the base material was about 3.9 µm, as shown in Figure 14 where Figure 14(A) showed the microstructure from a top surface while Figure 14(B) from a cross-section view.

The welding zone creates heat higher than the melting temperature and then rapid cooling. Under the heat produced by resistance and welding current, the fusion zone and heat-affected zone are heated above the critical temperature, and ferrite starts to transform into austenite. The austenite changes into martensite throughout the cooling process. The microstructure of the nugget consists of columnar grains near the fusion line (elongated towards the center of the nugget zone) and small equiaxed grains inside the nugget. The heat-affected zone (HAZ) near the fusion line is predominantly tempered martensite. This is due to high temperature during the welding and rapid cooling of more than 1000℃/S which converts the base material microstructure to martensite with some bainite. As a result, the martensite volume fraction decreases from the nugget toward the base metal. The base material's microstructure was not changed during the welding process, as shown in Figures 15 and Figure 16 (a-e) which represntned the FESEM for diffrernt welding zone.

The microhardness results showed that the maximum hardness for both nuggets was in the nugget zone. In the heat-affected zone, and finally, in the base material, the maximum temperature was in the center of the nugget zone. It decreased slightly away from the center of the nuggets. The maximum hardness for the first nugget was 407 HV while for the second nugget was 365 HV, and this difference was also because of the shunt effect phenomenon, which reduced the amount of welding current that entered the second nugget and subsequently decreased the heat input to the second nugget as shown in Figure17.

Table 6: ANOVA for Tensile strength results

Source	DF	Seq SS	Adj SS	Adj MS	F	P	Contribution ratio %
current	2	63768067	63768067	31884033	6.48	0.134	79.76
time	2	1660161	1660161	830080	0.17	0.856	2.07
force	2	4673675	4673675	2336837	0.47	0.678	5.84
Residual Error	2	9843675	9843675	4921837			12.31
Total	8	79945578					

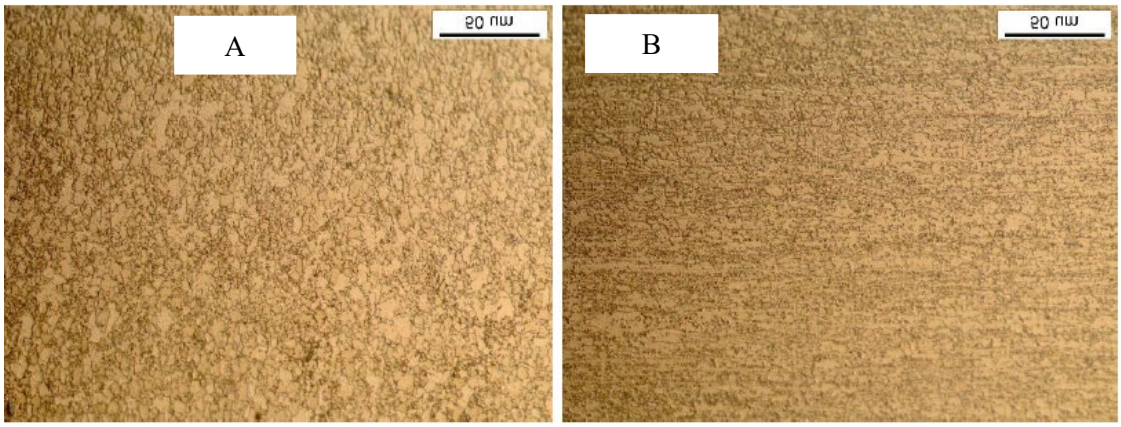

Figure 14: A top surface. B cross-section

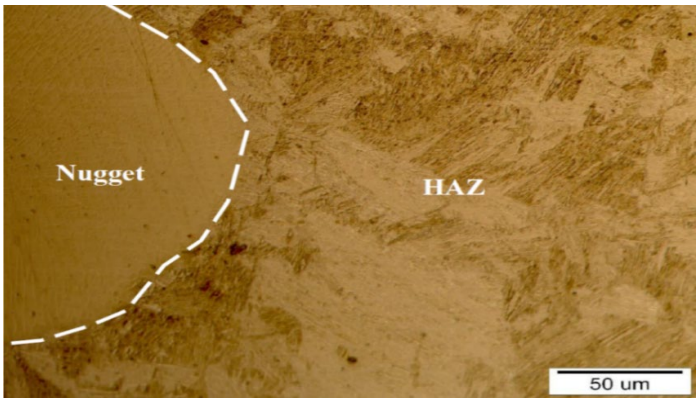

Figure 15: Optical micrograph of the interface of nugget zone and HAZ

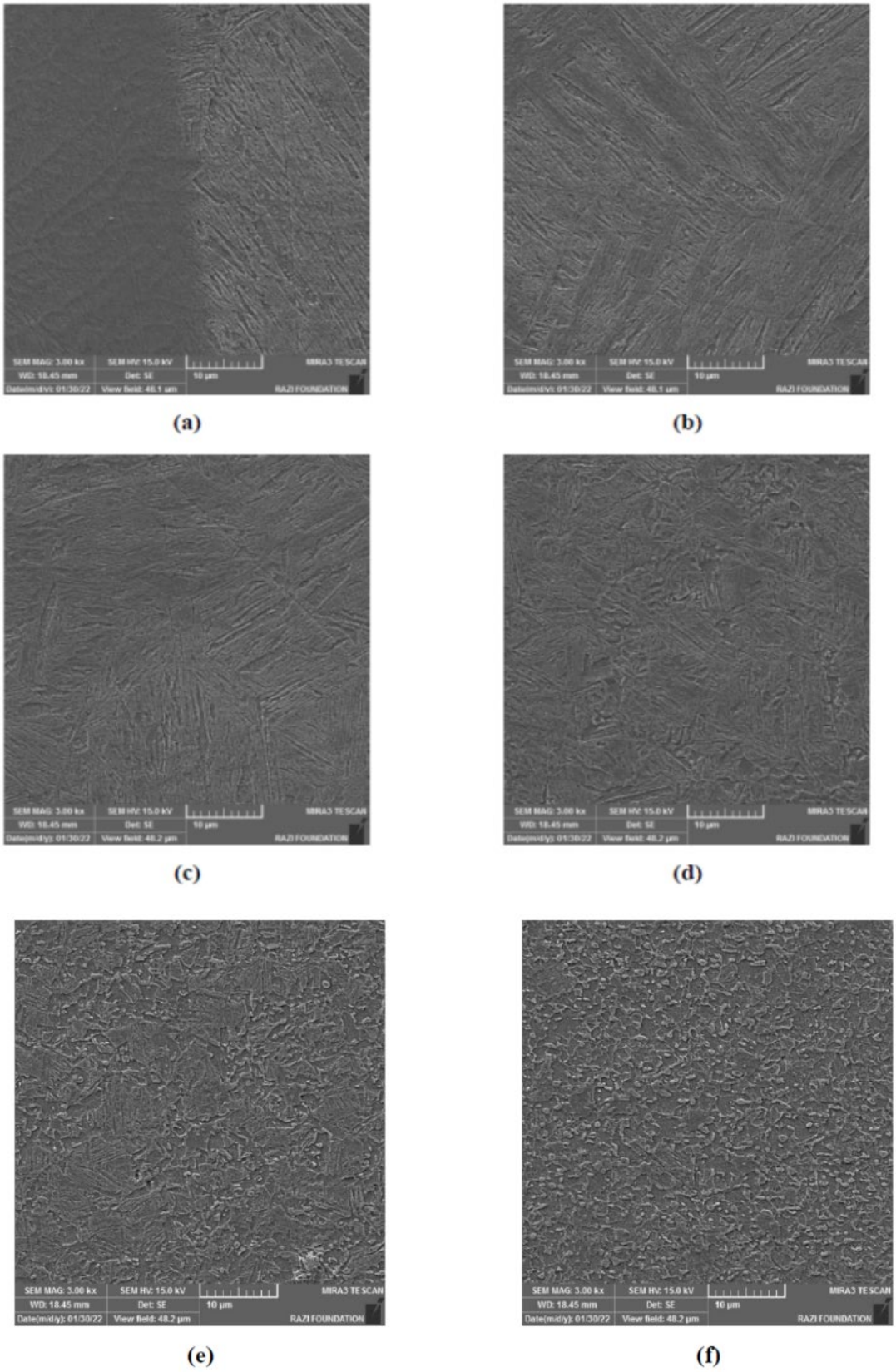

Figure 16: Microstructure of welded sample (a) nugget-HAZ interface; (b) to (e) from the HAZ towards the BM; (f) BM

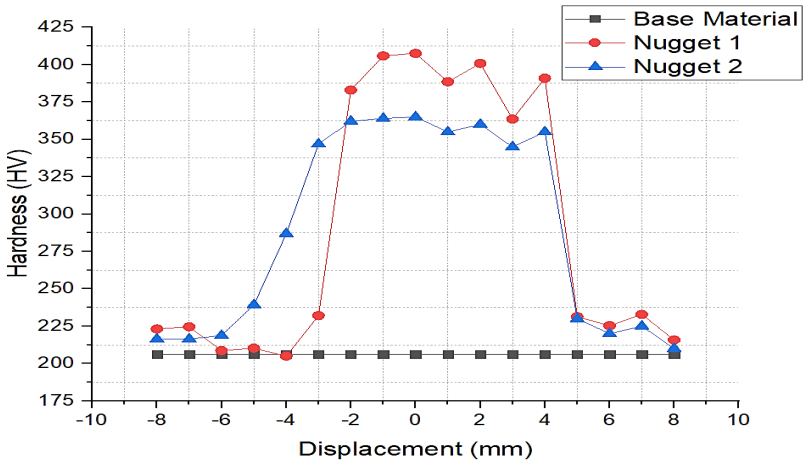

Figure 17: Microhardness test result

4. Conclusion

This paper presented an optimization process of resistance spot welding for high strength low alloy steel DOCOL 500 LA. The mechanical properties and microstructure of the nugget, HAZ, and base material were investigated. The main conclusions can be summarized below:

1) The optimum welding parameters were a welding current of 8800 Amp, welding time of 20 cycles, and electrode force of 1900 N.
2) The most effective welding parameters were welding current, electrode force, and welding time.
3) The shunting phenomenon significantly affects double spot welding by reducing the heat input to welded parts. This reduces the nugget diameter of second spots and decreases the strength of spot welding, so it is recommended that the distance between the center of two nuggets must be more than 20 mm to reduce the effect of the shunting phenomenon.
4) The microstructure for the nugget zone equiaxed grains towards the center of the nugget where the maximum temperature happened, and for HAZ was the martensite phase.
5) The microhardness value was maximum in the nugget zone, heat-affected zone, and finally in the base material because of the rapid melting and solidification in the nugget zone.

Acknowledgment

The authors would like to express their gratitude to SSAB company for steel manufacturing in Sweden for supplying the steel sheets to achieve this paper.

Author contribution

All authors contributed equally to this work.

Funding

This research received no specific grant from any funding agency in the public, commercial, or not-for-profit sectors.

Data availability statement

The data that support the findings of this study are available on request from the corresponding author.

Conflicts of interest

The authors declare that there is no conflict of interest.

References

[1] H. L. Jaber, M. Pouranvari, R. K. Salim, F. A. Hashim, S.P.H Marashi, Peak load and energy absorption of DP600 advanced steel resistance spot welds, Ironmak. Steelmak., 44 (2017) 699–706. https://doi.org/10.1080/03019233.2016.1229880

[2] Y.J. Chao, K.Wang, K.W Miller, X.K Zhu, Dynamic Separation of Resistance Spot Welded Joints: Part I—Experiments, Exp. Mech., 50 (2010) 889–900. https://doi.org/10.1007/s11340-009-9276-z

[3] M. Pouranvari, S. Sobhani, F.Goodarzi, Resistance spot welding of MS1200 martensitic advanced high strength steel: Microstructure-properties relationship. J. Mfg. Process., 31 (2018) 867–874. https://doi.org/10.1016/j.jmapro.2018.01.009

[4] D. Ren, D. Zhao, K. Zhao,L. Liu, Z, He. Resistance ceramic filled annular welding of DP980 high-strength steel, Mater. Des., 183 (2019) 108118 . https://doi.org/10.1016/j.matdes.2019.108118

[5] M .Pouranvari, S. P. H. Marashi, Critical review of automotive steels spot welding: process, structure and properties, Sci. Technol. Weld. Join., 18 (2013) 361–403. https://doi.org/10.1179/1362171813Y.0000000120

[6] A. Al-Mukhtar, Review of Resistance Spot Welding Sheets: Processes and Failure Mode, Adv. Eng. Forum, 17(2016). 31–57. https://doi.org/10.4028/www.scientific.net/AEF.17.31

[7] M. Marya, K.Wang, L. G. Hector, X. Gayden, Tensile-Shear Forces and Fracture Modes in Single and Multiple Weld Specimens in Dual- Phase Steels, J. Mfg. Sci. Eng., 128 (2006) 287-298. https://doi.org/10.1115/1.2137751

[8] S. D. Bolboacă, L. Jäntschi, Design of Experiments: Useful Orthogonal Arrays for Number of Experiments from 4 to 16, Entropy, 9 (2007) 198-232. https://doi.org/10.3390/e9040198

[9] S. K. Hussein, O. S. Barrak , Optimization the Resistance Spot Welding Parameters of Austenitic Stainless Steel and Aluminum Alloy Using Design of Experiment Method, Eng. Technol. J., 34 (2016) 1383-1401. https://doi.org/10.30684/etj.34.7A.11

[10] S. M. Hassonia, O. S. Barraka, M. I. Ismaila, S. K. Hussein. Effect of Welding Parameters of Resistance Spot Welding on Mechanical Properties and Corrosion Resistance of 316L. Mater. Res., 25 (2022). https://doi.org/10.1590/1980-5373-MR-2021-0117

[11] N. A. M. Yasin, A. Alisibramulisi, Z. Salleh, F. A. Ghazali, A. Pawan, Optimization of Resistance Spot Welding (RSW) Parameters by using Taguchi Method, Int. J. Innovative Technol. Exploring Eng., 9 (2020) 2795-2800. https://doi.org/10.35940/ijitee.C9215.019320